

# Virtual Lung Screening Trial (VLST): An *In Silico* Replica of the National Lung Screening Trial for Lung Cancer Detection

Fakrul Islam Tushar<sup>1,2</sup>, Liesbeth Vancoillie<sup>1</sup>, Cindy McCabe<sup>1,3</sup>, Amareswararao Kavuri<sup>1</sup>,  
Lavsén Dahal<sup>1,2</sup>, Brian Harrawood<sup>1</sup>, Milo Fryling<sup>1</sup>, Mojtaba Zarei<sup>1,2</sup>, Saman Sotoudeh-Paima<sup>1,2</sup>,  
Fong Chi Ho<sup>1,2</sup>, Dhrubajyoti Ghosh<sup>4</sup>, Sheng Luo<sup>4</sup>, W. Paul Segars<sup>1,2,3</sup>, Ehsan Abadi<sup>1,2,3</sup>,  
Kyle J. Lafata<sup>1,2,3,5</sup>, Joseph Y. Lo<sup>1,2,3\*</sup>, Ehsan Samei<sup>1,2,3\*</sup>

<sup>1</sup> Center for Virtual Imaging Trials, Carl E. Ravin Advanced Imaging Laboratories, Dept. of Radiology, Duke University School of Medicine

<sup>2</sup> Dept. of Electrical & Computer Engineering, Pratt School of Engineering, Duke University

<sup>3</sup> Medical Physics Graduate Program, Duke University

<sup>4</sup> Dept. of Biostatistics and Bioinformatics, Duke University School of Medicine

<sup>5</sup> Dept. of Radiation Oncology, Duke University School of Medicine.

\* These authors contributed equally as co-senior authors.

## Key Points

**Question:** Can virtual imaging trials replicate the outcomes of real-world lung cancer screening trials and provide valuable insights into the performance of CT and CXR for lung nodule detection?

**Findings:** This study created a virtual patient population to emulate the National Lung Screening Trial (NLST) and demonstrated that CT consistently outperformed chest X-ray (CXR) in detecting lung nodules. The virtual trial successfully mirrored key trends from the NLST, particularly the superior detection of larger nodules by CT, reinforcing its clinical relevance.

**Meaning:** The study's findings suggest that virtual imaging trials can effectively replicate real-world screening trials and serve as a reliable method for evaluating imaging technologies, offering a cost-effective, safe, and scalable alternative to traditional clinical trials.

## Abstract

**Importance:** Clinical imaging trials are crucial for definitive evaluation of medical innovations, but the process is inefficient, expensive, and ethically-constrained. Virtual imaging trial (VIT) approach address these limitations by emulating the components of a clinical trial. An *in silico* rendition of the National Lung Screening Trial (NLST) via Virtual Lung Screening Trial (VLST) demonstrates the promise of VITs to expedite clinical trials, reduce risks to subjects, and facilitate the optimal use of imaging technologies in clinical settings.

**Objectives:** To demonstrate that a virtual imaging trial platform can accurately emulate a major clinical trial, specifically the National Lung Screening Trial (NLST) that compared computed tomography (CT) and chest x-ray (CXR) imaging for lung cancer screening.

**Design, Setting, and Participants:** A diverse virtual patient population of 294 subjects was created from human models (XCAT) emulating the characteristics of cases on NLST, with two types of simulated lung nodules. The cohort was assessed using simulated CT and CXR systems to generate images that reflect the NLST imaging technologies. Deep learning models trained for lesion detection in CXR and CT served as virtual readers.

**Main Outcomes and Measures:** The primary outcome was the difference in the Receiver Operating Characteristic Area Under the Curve (AUC) for CT and CXR modalities. Lesion-level AUC was aggregated to report patient-level AUC.

**Results:** The study analyzed 294 CT and CXR simulated images from 294 virtual patients, with a lesion-level AUC of 0.81 (95% CI: 0.79-0.84) for CT and 0.56 (95% CI: 0.54-0.58) for CXR. At the patient level, CT demonstrated an AUC of 0.84 (95% CI: 0.80-0.89), compared to 0.52 (95% CI: 0.45-0.58) for

CXR. Subgroup analyses on CT results indicated superior detection of homogeneous lesions (lesion-level AUC 0.97) than heterogeneous lesions (lesion-level AUC 0.72). Performance was particularly high for identifying larger nodules (AUC of 0.98 for nodules > 8 mm). The VLST results closely mirrored the NLST, particularly in size-based detection trends, with CT achieving high AUCs for nodules  $\geq$  8 mm and similar challenges in detecting smaller nodules.

**Conclusion and Relevance:** The VIT results closely replicated those of the earlier NLST, underscoring its potential to replicate real clinical imaging trials. Integration of virtual trials may aid in the evaluation and improvement of imaging-based diagnosis.

## Introduction

Lung cancer ranks as the leading cause of cancer-related deaths, accounting for approximately 1.8 million fatalities in 2020.<sup>1,2</sup> Projections from the American Cancer Society indicate that an estimated 238K individuals in the United States are anticipated to be diagnosed with lung cancer in 2023.<sup>3</sup> In the realm of timely detection and diagnosis of lung cancer, imaging modalities like chest X-rays (CXR) and Computed Tomography (CT) scans play a crucial role for not only the diagnosis of lung cancer but also those of a wide range of abnormalities.<sup>4</sup>

Associating the early-state cancer detection to the larger likelihood of cure, multiple lung cancer screening trials worldwide have contributed valuable insights into the efficacy of lung cancer screening, such as National Lung Screening Trial (NLST),<sup>4</sup> Nederlands-Leuvens Longkanker Screenings Onderzoek (NELSON),<sup>5</sup> Multicentric Italian Lung Detection (MILD),<sup>6</sup> British Thoracic Society Lung Cancer Screening Group (BTSLSG),<sup>7</sup> and International Early Lung Cancer Action Program (IE-LCAP) trial.<sup>8</sup> In spite of their benefits, clinical trials are extraordinarily inefficient and costly. Over its duration of 8 years, for example, NLST enrolled over 50,000 subjects at a cost of \$256 million.<sup>9</sup> At the conclusion of such trials, the diagnosis or treatment being evaluated may already be obsolete. For medical imaging, that risk is particularly high because technology evolves so rapidly. Additionally, clinical trials may involve

putting patients at risk, including that of radiation exposure or overdiagnosis leading to unnecessary procedures. Therefore, it is imperative to develop alternative trial procedures that can address these gaps to ensure financial feasibility, timely change of clinical practice, and patient safety.<sup>10</sup>

Virtual Imaging Trials (VITs) leverage advances in computational techniques to simulate the workflow of clinical imaging trials, i.e., patients undergoing scans that are interpreted by readers. Compared to clinical trials, VITs may serve as an alternative that is faster, safer, and more cost-effective. In a trailblazing study, FDA scientists conducted a VIT to emulate a comparative clinical trial of two imaging modalities for breast cancer screening.<sup>11</sup> In their comprehensive review paper, Abadi *et al.* delve extensively into VITs in numerous imaging modalities to study myriad applications such as for coronavirus disease (COVID-19), emphysema, and organ dosimetry.<sup>12</sup> However, there are still very few VIT studies that emulate an end-to-end trial, however, due to the immense complexity of simulating all trial aspects. The most mature VIT studies to date have focused on breast cancer screening. To advance VIT applications, simulation software modules need to be integrated to facilitate research that is both expedient and rigorous, and the trials need to expand to other clinical settings with high clinical impact.

To address these gaps, this Virtual Lung Screening Trial (VLST) study aimed to undertake an “*in silico*” emulation of the NLST study to compare efficacy of CXR and CT in lung cancer screening. NLST was extremely important in medical imaging as it changed the clinical practice and led to the adoption of current lung cancer screening programs. Our VLST study presents three primary advances. First, patient-informed human models were used to generate a virtual patient population that reflects the demographics of the cancer detection cohort. Reflecting the challenging clinical task, the human models encompass the many anatomical structures of the chest and multiple types of lung nodules. Second, this study implemented virtual scanners for CXR and CT, modalities that have attracted considerable recent attention in machine learning research due to their high clinical volume and impact.<sup>13,14</sup> Specifically, these imaging techniques were implemented to create virtual images that align with the legacy NLST imaging technology. Finally, to complete the end-to-end trial, the detection task was executed through virtual readers leveraging established deep learning models trained on public patient data, thus providing robust

performance while ensuring reproducibility. By integrating these software modules, this study presented the first end-to-end virtual imaging trial in the new domain of chest imaging, designed to gauge the precision and efficacy of the virtual imaging trial platform for a task with high clinical relevance.

## Methods

### Study Design

**Figure 1** shows an overview of the different steps performed to accomplish the VLST comprised of simulating a virtual population, modeling virtual scanners, developing virtual readers, and finally analyzing the detection and diagnosis performance. In the section below, we will briefly explain each of these steps.

### Virtual Population

In any clinical trial, the selection of the targeted population and sample groups is of utmost importance, as it directly influences the validity of trial results and outcomes. The composition of the VIT population cohort was established through power calculations to replicate the outcomes of NLST, which are detailed in **eAppendix 1**.

The creation of a virtual human subject involved two key steps: constructing the normal anatomy followed by insertion of the specific abnormalities. For the VLST, the subjects employed were computational human models generated from full body CT scans from a single health system (Duke Health) which encompasses multiple hospitals. The construction of these human models involved a series of steps: beginning with the segmentation of specific organs, ensuring the quality control of these segmentations, followed by the creation of airways and vessels, and culminating in the voxelization process. An outline of this procedure is shown in **Figure 1**, with further information available in our previous publication.<sup>15</sup> In this research, we employed both pre-existing and newly developed 4D extended cardiac-torso (XCAT) models representing both sexes at varying age, height, weight, BMI, and race combinations.<sup>15-17</sup> Demographically, the mean age was 59.5 years, with a distribution between male (55.7%) and female (44.4%) participants. An earlier study evaluated the similarity between the NLST and

VLST datasets, finding no significant distributional differences in demographic variables, suggesting they can be used interchangeably for training and testing in virtual imaging trials.<sup>18</sup>

Simulated nodules were generated in two steps. First, a single-density lesion was formed, adhering to the desired morphology. Subsequently, a convolution process created a multi-density structure using a previously published approach.<sup>19,20</sup> Several instances of these simulated nodules, featuring diverse characteristics such as size and morphology, are depicted in **eFigure 1 and eFigure 2**. These simulated nodules were then randomly inserted into the lungs, guided by indications of where nodules have been observed in prior clinical trial studies.<sup>4</sup> A total of 512 lesions were created including 202 (39.4%) homogeneous and 310 (60.5%) heterogeneous lesions. Specifics regarding population demographics, along with inclusion and exclusion criteria, are clarified in **Table 1 and Figure 2**.

### Virtual Scanners and Imaging Protocols

The cohort of computational human models with nodules was virtually imaged using a validated imaging simulation tool (DukeSim).<sup>21-23</sup> DukeSim generates projection images from voxelized computational models using ray tracing (for primary signal) and Monte Carlo simulation (for scatter signal and radiation dose). To create CXR images, we mimicked the post-processing to replicate the contrast, noise, and resolution of the chest radiography technology used in the NLST era. For CT, projections were reconstructed using a vendor-neutral reconstruction tool (MCR toolkit)<sup>24</sup> with weighted filter back projection configured to mimic the physical and geometrical characteristics of two generic CT scanners, named Duke Legacy W12 and Duke Legacy W20, which are representative of NLST CT methods.<sup>25</sup> The geometry and acquisition configurations of the scanners are listed in **eTable 3**. Sample of human model and simulated images with lesions are presented in **Figure 3**.

### Virtual Reader

The virtual reader component of our study deployed deep learning models to emulate the image interpretation by radiologists. Two RetinaNet models were developed: a 2D model for CXR images and a

3D model for CT volumes.<sup>26</sup> This readily available machine learning architecture was trained with publicly accessible clinical datasets (LUNA16,<sup>27</sup> NODE2<sup>28</sup>) to ensure ease of replication and minimize virtual reader variability across a variety of diagnostic scenarios for both modalities. The architecture, training methodologies, and patch extraction techniques remained constant across both models, with only the training datasets and data dimensions varying. This approach is akin to having the same radiologist interpret different modalities with consistent training.

The workflow started with image data augmentation and utilized RetinaNet's feature pyramid network to extract multi-scale features.<sup>26</sup> Anchor boxes generated were matched with reference standard annotations provided with each public dataset, refined through regression, and classified to detect objects of interest.<sup>29</sup> The final predicted boxes were evaluated against the reference standard.<sup>26,29</sup> By incorporating such a model, we aimed to closely replicate the decision-making process of radiologists who search for initial lesion candidates, then use the most suspicious as the index lesion to inform follow-up recommendations. Detailed information regarding the development, validation, and the clinical datasets used for the virtual reader models is documented in **eAppendix 4**.

### **Trial End Point**

The evaluation of performance was conducted for lesion-level and patient-level detection. At the lesion level, each lesion was assessed individually. For patient-level evaluation, the lesion with the highest output value among all lesions within each patient represented performance on a per-patient basis.

Performance was assessed using the Receiver Operating Characteristic Area Under the Curve (AUC) at both the lesion and patient levels, with subgroup analyses for lesion type and size.

The VLST's primary endpoint was the difference in the Area Under the Curve (AUC) between CT and CXR for detection of lung nodules. Additionally, subgroup analyses were conducted to evaluate the AUC difference for two distinct lesion types and for lesions of varying sizes.



## Statistical Analysis

Performance was assessed using the AUC. The 95% confidence intervals (CIs) were calculated using the DeLong method with 2000 bootstrapping samples.<sup>30</sup>

## Results

In this VLST, virtual readers assessed 294 simulated CT scans and chest X-rays (CXR) originating from a cohort of 294 virtual human subjects. This cohort included 174 individuals with lung nodules and 139 without. The mean size (long axis) of these lesions was 10.09 mm, with a standard deviation of 5.09 mm, indicating variability in lesion sizes across the sample. The smallest lesion measured was 4 mm, while the largest lesion was 34 mm. The lesion sizes were distributed such that 25% of lesions were 6 mm or smaller (first quartile), the median size was 9 mm, and 75% of the lesions (third quartile) were 12 mm or larger.

At the lesion level, CT outperformed CXR with AUC of 0.81 (95% CI: 0.79-0.84) compared to 0.56 (95% CI: 0.54-0.58), reflecting a substantial difference between the two modalities. The patient-level evaluation showed even greater difference, with CT achieving AUC of 0.84 (95% CI: 0.80-0.89) relative to CXR's 0.52 (95% CI: 0.45-0.58).

Stratifying the results by lesion type and size revealed significant performance differences, but CT consistently outperformed CXR in each category. For the homogeneous lesion type, AUC for CT was 0.97 (95% CI: 0.95-0.98), substantially higher than for CXR at 0.66 (95% CI: 0.63-0.69). In contrast, for heterogeneous lesions, both modalities showed lower AUCs: CT 0.72 (95% CI: 0.67-0.76) versus CXR 0.52 (95% CI: 0.49-0.54). For lesion size, performance was much higher for the large nodules  $\geq 8$  mm, CT 0.98 (95% CI: 0.96-0.99) versus CXR 0.69 (95% CI: 0.65-0.73), compared to the smaller nodules  $< 8$  mm where both modalities were similarly poor: CT 0.57 (95% CI: 0.52-0.62) versus CXR 0.55 (95% CI: 0.50-0.60).

The NLST showed a 20% reduction in lung cancer mortality with LDCT vs. CXR, detecting 4+ mm non-calcified nodules. In the NLST, LDCT achieved a sensitivity of **93.1%** and specificity of **76.5%**, with an

AUC of **0.934**. Increasing the lesion size threshold to **6 mm** or **8 mm** significantly improved specificity, up to **92.0%**, with minimal reduction in sensitivity, highlighting the critical role of nodule size in lung cancer detection.<sup>31</sup> In our **VLST**, the mean lesion size was **10.09 mm**, aligning with NLST thresholds. CT outperformed CXR, especially for nodules  $\geq 8$  mm, where CT achieved an AUC of **0.98**, similar to NLST's high sensitivity and specificity. For smaller nodules ( $< 8$  mm), both modalities showed lower performance, with CT reaching an AUC of **0.57** compared to CXR's **0.55**, mirroring NLST's challenges. These results validate our virtual trial's ability to emulate NLST's size-based detection trends.

## Discussion

The main purpose of this study was to establish a VIT platform capable of emulating a major clinical trial in the modalities of CXR and CT imaging. To that end, this Virtual Lung Screening Trial for lung nodule detection replicated three fundamental elements of the real-world NLST study: patients, scanners, and readers. By simulating a diverse virtual patient population, utilizing validated radiologic simulators for imaging, and employing machine learning algorithms as standardized virtual readers, our approach provides robust comparison using each virtual subject as their own control, with completely reproducible experimental methods in the end-to-end trial process. Reflecting real-world radiological assessments, CT outperformed CXR in nodule detection.

The composition of the trial population stands as a pivotal element in the execution and success of any clinical study. The VICTRE trial, one of the first published virtual trial in breast imaging, represents a significant milestone within the realm of virtual imaging trials, exhibiting results that are promising when juxtaposed with those derived from human trials.<sup>11</sup> In comparison, our investigation demonstrated the trial effect while using a smaller virtual cohort based on a prior power analysis study than that of existing clinical lung screening studies.<sup>4,5,7</sup> Despite this, our study extended beyond the scope of prior VIT research, which typically focused on simulating specific pathologies or singular organs.<sup>11,12</sup> The construction of our trial population posed unique challenges to replicate the thoracic anatomy of a virtual human. To mirror the heterogeneity encountered in real-world clinical settings,<sup>4</sup> our study incorporated a

spectrum of age, sex, and race/ethnicity in attempt to reflect the diverse human population encountered in actual clinical trials.<sup>4</sup> Furthermore, we calibrated our virtual models to account for a range of lesion sizes and types. This diversity and clinical realism not only enhanced the relevance of our findings but also facilitated future research in complex bodily system simulations.

An advantage of DukeSim (virtual scanner) over physical scanners is its ability to simulate a wide range of imaging conditions and anatomical variations without the limitations of radiation exposure, patient variability, or scanner availability. This allows for more controlled experiments, rapid prototyping of imaging techniques, and optimization of screening protocols, all in a cost-effective and risk-free virtual environment, which is not feasible with physical scanners. Using virtual patients also allowed scanning the same patient with both modalities, thus using each patient as their own control to provide greater power, which would not be possible in the real world due to the increase in radiation risk.

The virtual readers were designed using established deep-learning libraries<sup>32</sup> and were trained on publicly available clinical datasets<sup>27,28</sup> to ensure that the development process remained reproducible and broadly applicable. Unlike traditional VITs, which typically employ mathematical observer models that evaluate specific imaging regions for the presence or absence of signal,<sup>11,33</sup> our virtual readers incorporated a search process.<sup>26</sup> This process mirrored the diagnostic approach of a radiologist to first detect and then characterize lesions. In previous VIT studies for COVID-19 detection, we showed that deep-learning models can be susceptible to training and testing biases, which were more pronounced for CXR systems with their great diversity of image appearances.<sup>34-36</sup> To minimize overtraining bias, we have deliberately avoided complex model architectures and elaborate training methodologies, thereby aligning the virtual readers' functionality as closely as possible with that of human readers across different imaging modalities. Reported results demonstrated that CT outperformed CXR in nodule detection, which was consistent with the performance seen in clinical lung cancer screening trials. Our simulated homogenous lesions performed higher detection performance in both modalities compared to the heterogeneous.

This study has several limitations. Although the number of virtual patients was relatively small, it was determined based on a prior power analysis study to ensure sufficient statistical power. For future work, our efforts will pivot towards enriching the virtual population with an even broader spectrum of diverse and underrepresented virtual subjects and additional lesion types. In terms of the virtual reader, only a single model was developed for each modality, which did not take into account the effects of reader variability. This can be addressed by using multiple models with different architectures and levels of training. Finally, like almost all other studies to date, our VIT focused only on the task of detection, which does not fully represent the impact of clinical trials that evaluate the patient-level endpoint outcomes as cancer risk or survival.<sup>4</sup> Although VLST provided patient-level detection, it is not straightforward to directly translate those results to NLST's patient-level endpoints, which are driven by not only imaging findings discernible by radiologists or virtual readers but also additional information such as current pathologic diagnosis and eventual outcomes that occur years later. However, our VLST closely mirrors the findings of the NLST, particularly in the size-based detection of lung nodules. Both trials demonstrate that CT is highly effective for detecting larger nodules, with performance declining for smaller nodules. The similarity between VLST and NLST highlights the ability of our virtual trial to accurately emulate real-world screening scenarios. Recognizing this limitation, our future research aims to expand VITs to more closely replicate clinical trial scenarios by considering patient-level outcomes, such as cancer diagnoses, to enhance the clinical relevance of VITs.

In conclusion, this study presented one of the first end-to-end VITs in the domain of chest imaging, which involve the use of CXR and CT modalities. These modalities are the subject of considerable research interest due to their high clinical volume and impact. Together, the complexity of human models, versatility of scanners, and robustness of readers contribute to the advancement of virtual trials for complex bodily systems and imaging challenges. The transformative potential of virtual imaging trials in

advancing evidence-based medicine offers an efficient and ethically conscious approach to medical research and development.

## **Acknowledgments**

This work was funded in part by the National Institutes of Health (P41-EB028744, R01EB001838, R01HL155293).

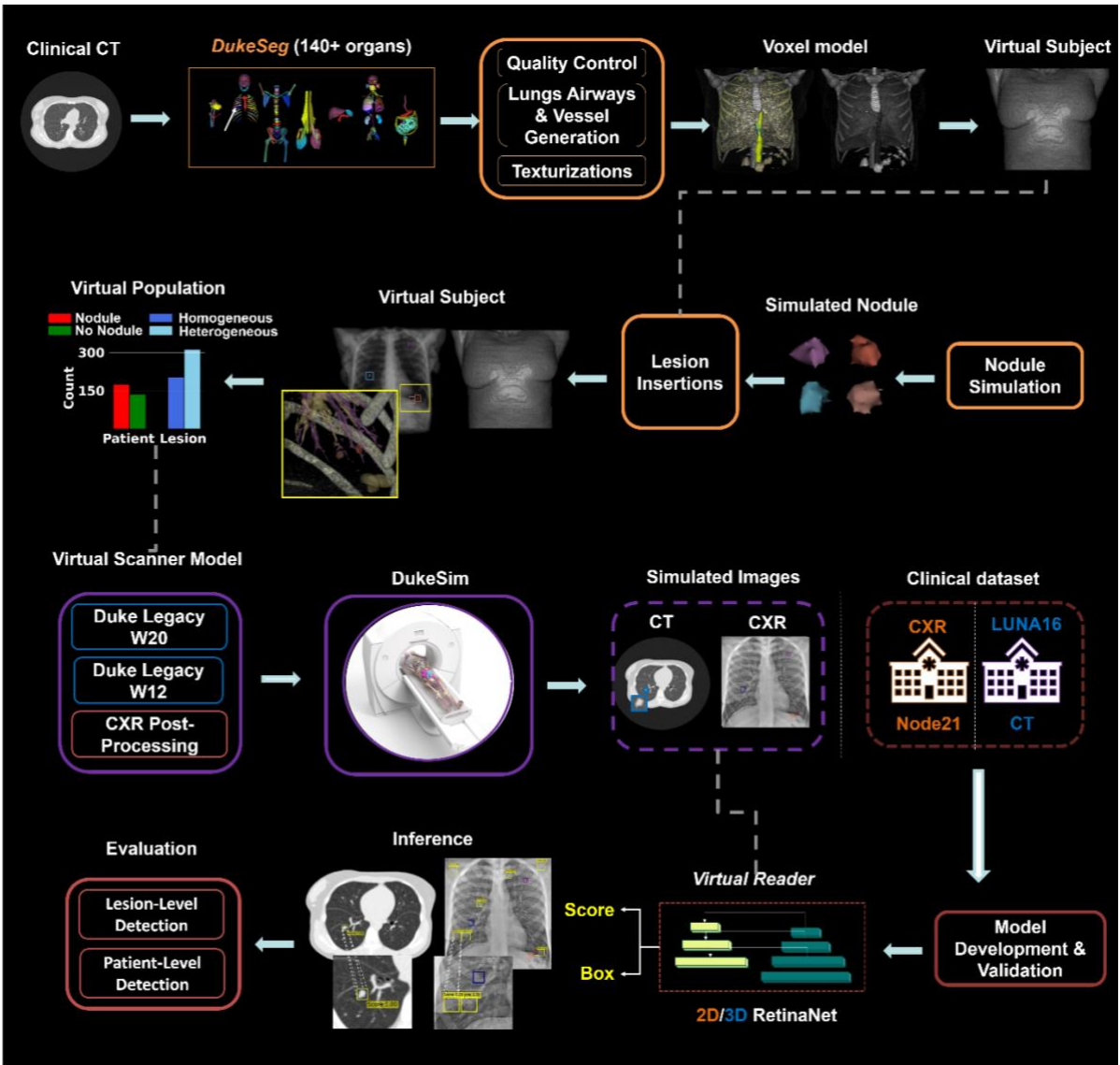


**Figure 1.** Flowchart summarizing the comprehensive workflow of the Virtual Lung Screening Trial (VLST), from creation of virtual patient models using clinical CT data, through lesion simulation and insertion, to virtual imaging using DukeSim, and concluding with evaluation by a virtual reader employing 2D/3D RetinaNet for both lesion-level and patient-level detection evaluation.

**Table 1. Cohort Characteristics of the VLST Virtual Population of With Cases Corresponding to with and without simulated nodule.**

<b>Characteristics</b>	<b>All</b>	<b>With Lung Nodule (n=174)</b>	<b>Without Lung Nodule (n=87)</b>
<b>Age (year)</b>			
Mean ± Std	59 ± 14	59 ± 15	60 ± 13
<b>Sex</b>			
Male	145 (55.56%)	95 (54.60%)	50 (57.47%)
Female	116 (44.44%)	79 (45.40%)	37 (42.22%)
<b>Weight (kg)</b>			
Mean ± Std	78± 20	77 ± 20	80 ± 20
<b>BMI</b>			
Mean ± Std (min-max)	27± 6 (13-50)	26± 6 (13-50)	28 ± 5 (18-41)
<b>Race</b>			
White	196 (75.10 %)	128 (73.56%)	68 (78.16%)
Black or African American	55 (21.07%)	36 (20.69%)	19 (21.84%)

Other/Unknown	10 (3.83%)	10 (5.75 %)	
<b>Ethnic</b>			
Not Hispanic or Latino	257 (98.47%)	171 (98.28%)	86 (98.85 %)
Hispanic/ Unknown	4 (1.53 %)	3 (1.73 %)	1 (1.15%)

**\*Note: Characteristics for the existing 33 without lung nodule human models are currently unavailable.**



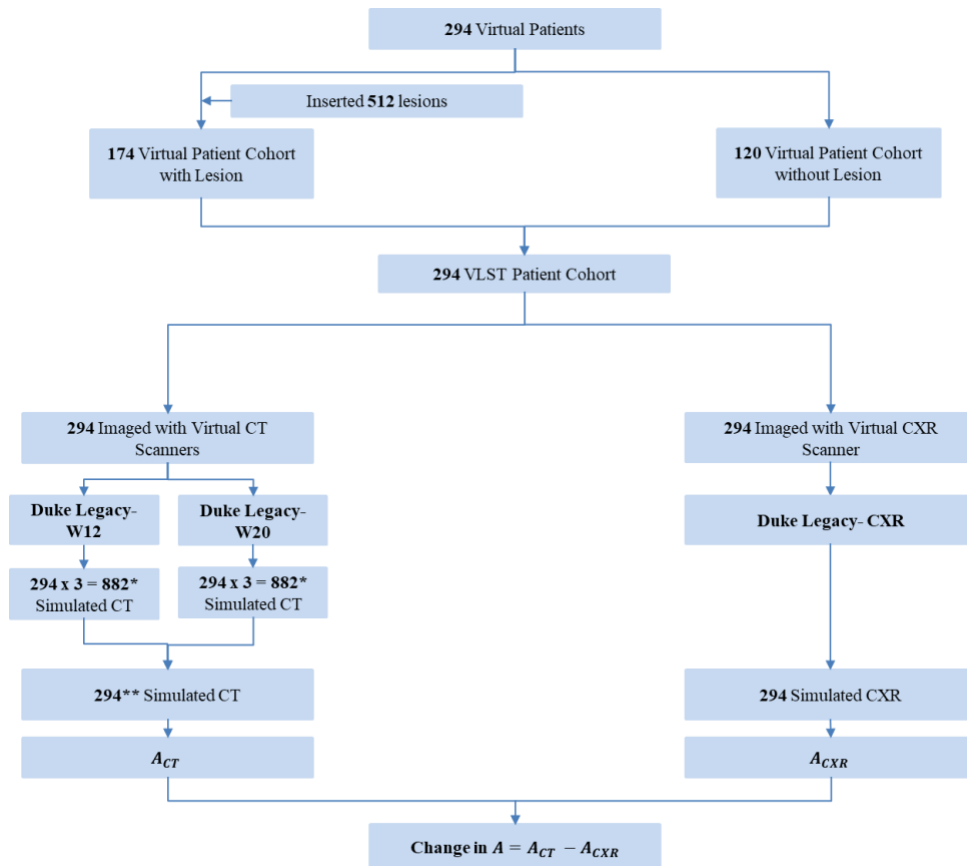
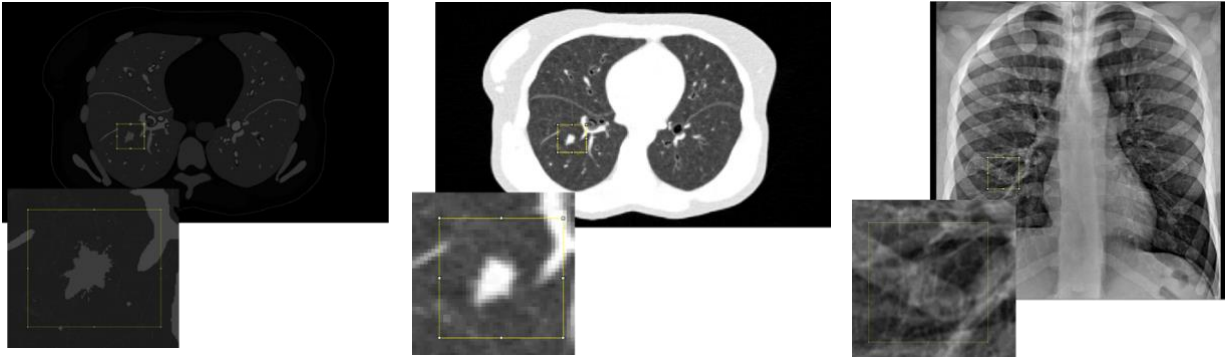


**Figure 2.** Virtual Patient’s inclusion and exclusion criteria and progress through the study. Within the study, 294 virtual patients were assessed, with 174 of them having a total of 512 lesions, varying from homogeneous to heterogeneous in nature. All 294 virtual patients underwent both virtual CT and CXR scans. For the CT cohort, \*294 virtual images were processed through two distinct scanners, the Duke Legacy-12 and the Duke Legacy-20, with each scanner producing three unique imaging configurations per patient (294 x 3=882). \*\*From these six configurations, one CT image per patient, total 294 was randomly selected for evaluation. As for the CXR cohort, all 294 virtual patients were successfully imaged using the Duke Legacy-CXR scanner. A indicate the area under the receiver operating characteristic curve.



(a) Human Model

(b) Simulated CT

(c) Simulated CXR

**Figure 3.** Example of human model and simulated images from the Virtual Lungs Screening Trial. Selected slice of (A) computation human model with a homogenous lesion (B) simulated CT scan image from Duke Legacy W20 scanner C) simulated CXR image using legacy post-processing.

**Table. 2: VLST End Points (AUC and Change in AUC) for the CT and CXR in lesion and patient-level, sub-group analysis with lesion type and lesion size (largest axis).**

VLST	AUC (95% CI)		p-value
	CT	CXR	
Lesion-level	0.81 (0.79-0.84)	0.56 (0.54-0.58)	< 0.001
Patient-level	0.84 (0.80-0.89)	0.52 (0.45- 0.58)	< 0.001
<b>By lesion-type</b>			
Homogeneous lesion (n=202)	0.97 (0.95-0.98)	0.66 (0.63-0.69)	< 0.001
Heterogeneous lesion (n=310)	0.72 (0.67-0.76)	0.52 (0.49-0.54)	< 0.001
<b>By lesion-size</b>			
Nodule < 8 mm (n=79)	0.57 (0.52-0.62)	0.55 (0.50-0.60)	0.6
Nodule ≥ 8 mm (n=433)	0.98 (0.96-0.99)	0.69 (0.65-0.73)	< 0.001

## References

1. Ferlay J, Colombet M, Soerjomataram I, et al. Cancer statistics for the year 2020: An overview. *International Journal of Cancer*. 2021;149(4):778-789. doi:10.1002/ijc.33588
2. Sung H, Ferlay J, Siegel RL, et al. Global Cancer Statistics 2020: GLOBOCAN Estimates of Incidence and Mortality Worldwide for 36 Cancers in 185 Countries. *CA: A Cancer Journal for Clinicians*. 2021;71(3):209-249. doi:10.3322/caac.21660
3. Siegel RL, Miller KD, Wagle NS, Jemal A. Cancer statistics, 2023. *Ca Cancer J Clin*. 2023;73(1):17-48.
4. Reduced Lung-Cancer Mortality with Low-Dose Computed Tomographic Screening. *New England Journal of Medicine*. 2011;365(5):395-409. doi:10.1056/nejmoa1102873
5. De Koning HJ, Van Der Aalst CM, De Jong PA, et al. Reduced Lung-Cancer Mortality with Volume CT Screening in a Randomized Trial. *New England Journal of Medicine*. 2020;382(6):503-513. doi:10.1056/nejmoa1911793

6. Pastorino U, Sverzellati N, Sestini S, et al. Ten-year results of the Multicentric Italian Lung Detection trial demonstrate the safety and efficacy of biennial lung cancer screening. *European Journal of Cancer*. 2019;118:142-148. doi:10.1016/j.ejca.2019.06.009
7. Field JK, Duffy SW, Baldwin DR, et al. The UK Lung Cancer Screening Trial: a pilot randomised controlled trial of low-dose computed tomography screening for the early detection of lung cancer. *Health Technology Assessment*. 2016;20(40):1-146. doi:10.3310/hta20400
8. Welch HG, Woloshin S, Schwartz LM, et al. Overstating the Evidence for Lung Cancer Screening. *Archives of Internal Medicine*. 2007;167(21):2289. doi:10.1001/archinte.167.21.2289
9. National Cancer I. National Lung Screening Trial (NLST). 2024/09/03 2024;
10. Heleno B, Thomsen MF, Rodrigues DS, Jørgensen KJ, Brodersen J. Quantification of harms in cancer screening trials: literature review. *BMJ : British Medical Journal*. 2013;347:f5334. doi:10.1136/bmj.f5334
11. Badano A, Graff CG, Badal A, et al. Evaluation of Digital Breast Tomosynthesis as Replacement of Full-Field Digital Mammography Using an In Silico Imaging Trial. *JAMA Network Open*. 2018;1(7):e185474. doi:10.1001/jamanetworkopen.2018.5474
12. Abadi E, Segars W, Tsui BM, et al. Virtual clinical trials in medical imaging: a review. *Journal of Medical Imaging*. 2020;7(4):042805.
13. Hamamci IE, Er S, Almas F, et al. A foundation model utilizing chest CT volumes and radiology reports for supervised-level zero-shot detection of abnormalities. *arXiv preprint arXiv:240317834*. 2024;
14. Chambon P, Delbrouck J-B, Sounack T, et al. CheXpert Plus: Hundreds of Thousands of Aligned Radiology Texts, Images and Patients. *arXiv preprint arXiv:240519538*. 2024;
15. Lavsén D, Yuqi W, Fakrul Islam T, et al. Automatic quality control in computed tomography volumes segmentation using a small set of XCAT as reference images. 2023:1246342.
16. Segars WP, Bond J, Frush J, et al. Population of anatomically variable 4D XCAT adult phantoms for imaging research and optimization. *Medical Physics*. 2013;40(4):043701. doi:10.1118/1.4794178
17. Data from: American Association of Physicists in Medicine, Truth-Based CT (TrueCT) Reconstruction Challenge
18. Ghosh D, Lo J, Vancoillie L, Tushar FI, Dahal L, Samei E. Generalized Methodologies for Assessing the similarity and dissimilarity between two datasets. *arXiv preprint arXiv:2405.05359*; 2024:248.
19. Sauer TJ, Bejan A, Segars P, Samei E. Development and CT image-domain validation of a computational lung lesion model for use in virtual imaging trials. *Medical Physics*. 2023;50(7):4366-4378. doi:<https://doi.org/10.1002/mp.16222>
20. McCabe C, Solomon J, Segars WP, Abadi E, Samei E. *Synthesizing heterogeneous lung lesions for virtual imaging trials*. vol 12925. SPIE Medical Imaging. SPIE; 2024.
21. Jadick G, Abadi E, Harrawood B, Sharma S, Segars WP, Samei E. A scanner-specific framework for simulating CT images with tube current modulation. *Physics in Medicine & Biology*. 2021;66(18):185010.

22. Abadi E, Harrawood B, Sharma S, Kapadia A, Segars WP, Samei E. DukeSim: A Realistic, Rapid, and Scanner-Specific Simulation Framework in Computed Tomography. *IEEE Transactions on Medical Imaging*. 2019;38(6):1457-1465. doi:/10.1109/tmi.2018.2886530
23. Abadi E, Paul Segars W, Chalian H, Samei E. Virtual Imaging Trials for Coronavirus Disease (COVID-19). *AJR Am J Roentgenol*. Feb 2021;216(2):362-368. doi:/10.2214/AJR.20.23429
24. Clark DP, Badea CT. MCR toolkit: A GPU-based toolkit for multi-channel reconstruction of preclinical and clinical x-ray CT data. *Medical Physics*. 2023;
25. Cagnon CH, Cody DD, McNitt-Gray MF, Seibert JA, Judy PF, Aberle DR. Description and implementation of a quality control program in an imaging-based clinical trial. Elsevier; 2006.
26. Lin T-Y, Goyal P, Girshick R, He K, Dollár P. Focal loss for dense object detection. 2017:2980-2988.
27. Setio AAA, Traverso A, De Bel T, et al. Validation, comparison, and combination of algorithms for automatic detection of pulmonary nodules in computed tomography images: The LUNA16 challenge. *Medical Image Analysis*. 2017;42:1-13. doi:10.1016/j.media.2017.06.015
28. Sogancioglu E, Murphy K, Ginneken Bv, Scholten E, Schalekamp S, Hendrix W. Data from: Node21. Grand Challenge Competition. 2021.
29. Zhang S, Chi C, Yao Y, Lei Z, Li SZ. Bridging the gap between anchor-based and anchor-free detection via adaptive training sample selection. 2020:9759-9768.
30. Boyd K, Eng KH, Page CD. Area under the precision-recall curve: point estimates and confidence intervals. Springer; 2013:451-466.
31. Pinsky PF, Gierada DS, Nath H, Kazerooni EA, Amorosa J. ROC curves for low-dose CT in the National Lung Screening Trial. *Journal of medical screening*. 2013;20(3):165-168.
32. Cardoso MJ, Li W, Brown R, et al. Monai: An open-source framework for deep learning in healthcare. *arXiv preprint arXiv:221102701*. 2022;
33. Samei E, Krupinski EA. *The handbook of medical image perception and techniques*. Cambridge University Press; 2018.
34. Tushar FI, Dahal L, Sotoudeh-Paima S, et al. Data diversity and virtual imaging in AI-based diagnosis: A case study based on COVID-19. *arXiv preprint arXiv:230809730*. 2023;
35. Tushar FI, Abadi E, Mazurowski MA, Segars WP, Samei E, Lo JY. Virtual vs. Reality: External Validation of COVID-19 Classifiers using XCAT Phantoms for Chest Computed Tomography. presented at: Proc Spie; 2022;
36. Dahal L, Tushar FI, Abadi E, et al. Virtual vs. Reality: External Validation of COVID-19 Classifiers using XCAT Phantoms for Chest Radiography. presented at: Medical Imaging 2022: Physics of Medical Imaging; 2022;